

Tetranuclear rhodium clusters with facial cyclooctatetraene ligands †

Hubert Wadepohl,* Rüdiger Merkel, Hans Pritzkow and Sven Rihm

Anorganisch-Chemisches Institut der Ruprecht-Karls-Universität, Im Neuenheimer Feld 270, D-69120 Heidelberg, Germany. E-mail: bu9@ix.urz.uni-heidelberg.de

Received 21st June 2001, Accepted 25th September 2001

First published as an Advance Article on the web 22nd November 2001

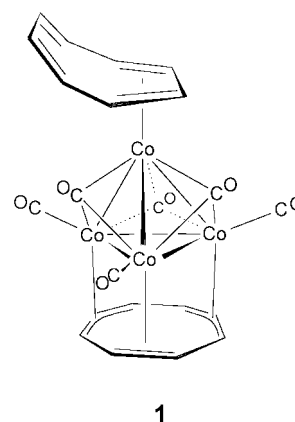
Molecular tetra-rhodium cluster complexes with facial (μ_3 -) cyclooctatetraene ligands are synthesized from $[\text{Rh}_4(\text{CO})_{12}]$ **2** and 1,3,5,7-cyclooctatetraene (cot) or 1,4-(SiMe_3)₂C₈H₆, respectively. The reactions proceed in a cooperative fashion, with all four metal atoms of the cluster being involved. Reaction of **2** with cot at low temperature (boiling *n*-pentane) only gives the mono-cot complex $[\text{Rh}_4(\text{CO})_8(\mu_3\text{-C}_8\text{H}_8)]$ **4**, whereas at higher temperature (boiling *n*-heptane) the bis-cot cluster complex $[\text{Rh}_4(\text{CO})_6(\mu_3\text{-C}_8\text{H}_8)(\eta^4\text{-C}_8\text{H}_8)]$ **5** is formed exclusively. Complex **4** is also prepared from **5** and $[\text{Fe}(\text{CO})_5]$. From **2** and 1,4-(SiMe_3)₂C₈H₆ in boiling *n*-pentane only the complex $[\text{Rh}_4(\text{CO})_6(\mu_3\text{-C}_8\text{H}_6(\text{SiMe}_3)_2)\{\eta^4\text{-C}_8\text{H}_6(\text{SiMe}_3)_2\}]$ **6** is obtained in quantitative yield. Substitution of the apical ligands in **4** with 1,4-(SiMe_3)₂C₈H₆, and in **5** with 1,3-cyclohexadiene or 1,5-cyclooctadiene gives the complexes $[\text{Rh}_4(\text{CO})_6(\mu_3\text{-C}_8\text{H}_8)\{\eta^4\text{-C}_8\text{H}_6(\text{SiMe}_3)_2\}]$ **7**, $[\text{Rh}_4(\text{CO})_6(\mu_3\text{-C}_8\text{H}_8)(\eta^4\text{-C}_6\text{H}_8)]$ **8** and $[\text{Rh}_4(\text{CO})_6(\mu_3\text{-C}_8\text{H}_8)(\eta^4\text{-C}_8\text{H}_{12})]$ **9**, respectively. The crystal and molecular structures of **4**, **5**, **6**, **8** and **9** were determined. The apical C₈H₆R₂ ligands in **5**, **6** and **7** attain the 1,2,5,6- η^4 -coordination mode through non-adjacent double bonds.

Introduction

Of the many bonding modes and hapticities available to the cyclic π -perimeters C_{*n*}H_{*n*}, the facial coordination mode has attracted considerable interest in recent years.¹ A very few examples of facial C_{*n*}H_{*n*} coordination in molecular cluster complexes have been known for quite a long time, e.g. facial cyclopentadienyl (*n* = 5) in $[(\eta\text{-C}_5\text{H}_5)\text{Rh}]_3(\mu_3\text{-H})(\mu_3\text{-}\eta\text{-C}_5\text{H}_5)]$ ² or facial cyclooctatetraene (*n* = 8) in $[(\text{CO})_2\text{Co}]_3(\mu_3\text{-CPh})(\mu_3\text{-}\eta^2\text{:}\eta^2\text{:}\eta^2\text{-C}_8\text{H}_8)]$.³ For a long time, such complexes were regarded mainly as laboratory curiosities lacking any further significance. However, with the advance of sophisticated surface analysis techniques⁴ in the 1980s it quickly became obvious that facial coordination is widespread in the adsorption states of C_{*n*}H_{*n*} on (especially close-packed) metal surfaces.⁵ The first reports, spectacular and still controversial, of a dramatic modification of the geometry and electronic structure of benzene upon adsorption⁶ were seminal for the development of the metal cluster chemistry of arenes. To date, a large number of molecular cluster complexes with facial benzene and benzene derivatives have been prepared and examined in much detail.⁷ The facial coordination mode of the larger cyclic polyenes has however received little attention, and only fairly recently a rich chemistry of facial hydrocarbon ligands beyond the arenes (*n* > 6) has been developed.¹

In contrast to a previous report,⁸ reaction of $[\text{Co}_4(\text{CO})_{12}]$ with 1,3,5,7-cyclooctatetraene (cot) was found to give the cluster complex $[\text{Co}_4(\text{CO})_6(\mu_3\text{-C}_8\text{H}_8)(\eta^4\text{-C}_8\text{H}_8)]$ **1** in excellent yield.⁹ In complex **1**, one of the cot ligands adopts the facial bonding mode, capping a tricobalt face of the cluster. A lot of chemical evidence suggests the M₃($\mu_3\text{-C}_8\text{H}_8$) arrangement to be a rather stable and kinetically inert chemical entity.^{9–12}

Reaction of $[\text{Rh}_4(\text{CO})_{12}]$ **2** with cot in boiling benzene was



reported to give a tetranuclear cluster complex of gross composition $[\text{Rh}_4(\text{CO})_8(\text{C}_8\text{H}_8)_2]$ **3**.⁸ Three possible structures were suggested for **3**, each one with two apical η^4 -coordinated cot ligands. Considering the sparseness of analytical data reported for **3** we decided to initiate a reinvestigation of this work. In the light of our results obtained with $[\text{Co}_4(\text{CO})_{12}]$, we felt that facial coordination would probably also dominate the coordination chemistry of $[\text{Rh}_4(\text{CO})_{12}]$ with cyclic polyenes.

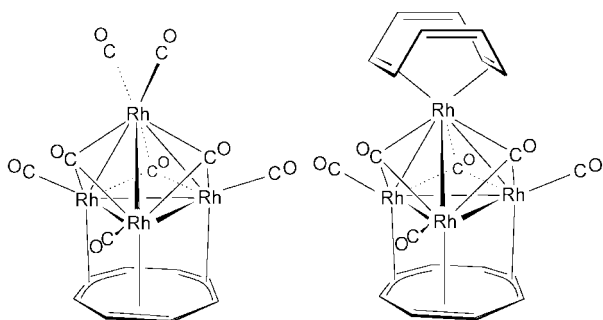
Results

(a) Synthetic studies

Reaction of $[\text{Rh}_4(\text{CO})_{12}]$ **2** with a large excess of cot in *n*-pentane gave a nearly quantitative yield of the mono-cot cluster complex $[\text{Rh}_4(\text{CO})_8(\mu_3\text{-C}_8\text{H}_8)]$ **4**. When the same reaction was carried out at a higher temperature (boiling *n*-heptane), the bis-cot cluster complex $[\text{Rh}_4(\text{CO})_6(\mu_3\text{-C}_8\text{H}_8)(\eta^4\text{-C}_8\text{H}_8)]$ **5** was formed exclusively. The yield of **5** could be maximized (up to 96%) by monitoring the IR spectrum of the reaction mixture and immediately stopping the reaction after all **2** had been consumed. Further heating was found to cause rapid

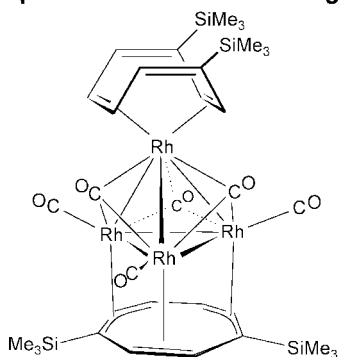
† Dedicated to Professor Hansgeorg Schnöckel on the occasion of his 60th birthday.

Electronic supplementary information (ESI) available: packing diagrams for **4** and **6**. See <http://www.rsc.org/suppdata/dt/b1/b105485f/>



4

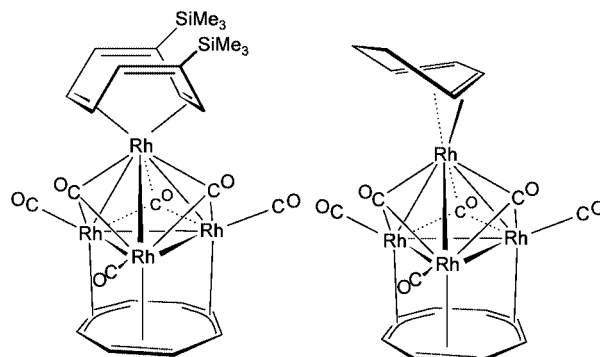
5



6

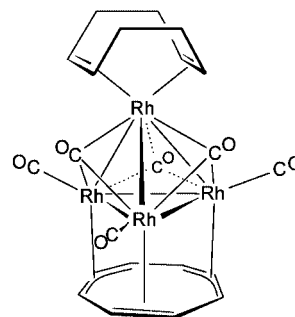
Table 1 IR (ν_{CO}) data (cm^{-1} , in CH_2Cl_2) for $[\text{Rh}_4(\text{CO})_6(\mu_3\text{-C}_8\text{H}_6\text{R}_2)\text{L}_2]$ **4** ($\text{R} = \text{H}$, $\text{L} = \text{CO}$), **5** ($\text{R} = \text{H}$, $\text{L}_2 = \text{C}_8\text{H}_8$), **6** ($\text{R} = \text{SiMe}_3$, $\text{L}_2 = \text{C}_8\text{H}_6(\text{SiMe}_3)_2$), **7** ($\text{R} = \text{H}$, $\text{L}_2 = \text{C}_8\text{H}_6(\text{SiMe}_3)_2$), **8** ($\text{R} = \text{H}$, $\text{L}_2 = \text{C}_6\text{H}_8$) and **9** ($\text{R} = \text{H}$, $\text{L}_2 = \text{C}_8\text{H}_{12}$)

	Terminal CO	Bridging CO
4	2080(s), 2032(vs), 2010(sh)	1780(s, br)
5	2031(sh), 2011(vs), 1993(vs)	1776(s), 1745(s)
6	2011(vs), 1993(vs)	1776(s), 1745(s)
7	2030(vs), 2010(vs), 2000(vs)	1765(s), 1738(s)
8	1997(vs)	1762(s), 1751(s)
9	2028(sh), 2006(s), 1993(s)	1766(s), 1741(s)



7

8



9

decomposition of **5** to give a black material, which was insoluble in common solvents. Both **4** and **5** precipitate from the reaction mixture and can be recrystallized from methylene chloride.

When an approximately 1 : 2 mixture of **2** and $\text{C}_8\text{H}_6(\text{SiMe}_3)_2$ was heated in boiling *n*-pentane, the cluster complex $[\text{Rh}_4(\text{CO})_6\{\mu_3\text{-C}_8\text{H}_6(\text{SiMe}_3)_2\}\{\eta^4\text{-C}_8\text{H}_6(\text{SiMe}_3)_2\}]$ **6** was formed in essentially quantitative yield. In contrast to the reactions with unsubstituted cyclooctatetraene this reaction proceeds in the homogeneous phase. IR-spectroscopic monitoring did not give evidence for the intermediate formation of appreciable quantities of a complex $[\text{Rh}_4(\text{CO})_8\{\mu_3\text{-C}_8\text{H}_6(\text{SiMe}_3)_2\}]$.

Heating of **4** to about 100 °C in the presence of cot or 1,4- $\text{C}_8\text{H}_6(\text{SiMe}_3)_2$ gave the cluster complexes **5** and $[\text{Rh}_4(\text{CO})_6(\mu_3\text{-C}_8\text{H}_8)\{\eta^4\text{-C}_8\text{H}_6(\text{SiMe}_3)_2\}]$ **7**, respectively, in excellent yields. Likewise, treatment of **5** with an excess of 1,3-cyclohexadiene and 1,5-cyclooctadiene gave the complexes $[\text{Rh}_4(\text{CO})_6(\mu_3\text{-C}_8\text{H}_8)(\eta^4\text{-C}_6\text{H}_8)]$ **8** and $[\text{Rh}_4(\text{CO})_6(\mu_3\text{-C}_8\text{H}_8)(\eta^4\text{-C}_8\text{H}_{12})]$ **9**, respectively, in good yield.

Transformation of the bis-cot complex **5** into the mono-cot complex **4** was achieved by treatment of **5** with $[\text{Fe}(\text{CO})_5]$. As a second product of this reaction, the mononuclear complex $[(\text{CO})_3\text{Fe}(\eta^4\text{-C}_8\text{H}_8)]$ was detected by spectroscopic means.

(b) Spectroscopic characterization

The constitution of the novel cluster complexes **4–9** was established by spectroscopic means and confirmed by crystal structure analyses (*vide infra*). In all cases only the molecular ions are detected in the field desorption mass spectra. The infrared (ν_{CO}) spectra show bands due to terminal and triply bridging carbonyl ligands (Table 1). The absorptions are rather broad and not well resolved.

The NMR spectra of **4–9** are summarized in Tables 2 and 3. The number and shape of the resonances are independent on the temperature in the range 200 K $\leq T \leq$ 300 K. The proton resonances of **4**, **5**, **8** and **9** were found to depend on the solvent. The resonances of the facial cot ligands are affected most, with shifts $\Delta\delta$ to higher field of -0.94 for **4**, -0.72 for **5**, -0.71 for **8** and -0.64 ppm for **9** on going from chloroform to benzene as solvent.

In all complexes with a facial C_8H_8 ligand (*i.e.* **4**, **5**, **7**, **8** and **9**) a sharp singlet is observed for this ligand both in the proton and carbon NMR spectra. The apical C_8H_8 ligand in **5** appears as two ^1H and two ^{13}C resonances, which are separated by 0.88 ppm (^1H , CDCl_3) and 42.8 ppm (^{13}C), respectively. The patterns of resonances due to the apical cyclohexadiene and cyclooctadiene ligands, respectively, in the complexes **8** and **9** are also straightforward.

The spectra of the complexes containing the silylated cyclooctatetraene ligand are more complicated. The assignment of the resonances given in Tables 2 and 3 for complexes **6** and **7** is based on chemical shift, and on spin–spin coupling to the ^{103}Rh nucleus for the metal-coordinated parts of the ligands. Owing to the low solubility of the complexes **4**, **5** and **8** some of the ^{13}C NMR resonances due to the carbonyl ligands could not be detected. Two such resonances ($\delta = 186$ and 227) are present in the spectra of each **6**, **7** and **9**.

(c) X-Ray crystal structure analyses of the cluster complexes $[\text{Rh}_4(\text{CO})_8(\mu_3\text{-C}_8\text{H}_8)]$ **4**, $[\text{Rh}_4(\text{CO})_6(\mu_3\text{-C}_8\text{H}_8)(\eta^4\text{-C}_8\text{H}_8)]$ **5**, $[\text{Rh}_4(\text{CO})_6(\mu_3\text{-C}_8\text{H}_8)(\eta^4\text{-C}_8\text{H}_6(\text{SiMe}_3)_2)]$ **7**, $[\text{Rh}_4(\text{CO})_6(\mu_3\text{-C}_8\text{H}_8)(\eta^4\text{-C}_6\text{H}_8)]$ **8**, $[\text{Rh}_4(\text{CO})_6(\mu_3\text{-C}_8\text{H}_8)(\eta^4\text{-C}_8\text{H}_{12})]$ **9** and $[\text{Rh}_4(\text{CO})_6\{\mu_3\text{-C}_8\text{H}_6(\text{SiMe}_3)_2\}\{\eta^4\text{-C}_8\text{H}_6(\text{SiMe}_3)_2\}]$ **6**

Single crystals were obtained from solutions of the complexes **4–9**. Crystal details are summarized in the Experimental section. Unfortunately, due to the poor quality of the dataset collected from **7**, the structure of this cluster could not be

Table 2 ^1H NMR data (δ , in CDCl_3) for $[\text{Rh}_4(\text{CO})_6(\mu_3\text{-C}_8\text{H}_6\text{R}_2)\text{L}_2]$ **4** ($\text{R} = \text{H}$, $\text{L} = \text{CO}$), **5** ($\text{R} = \text{H}$, $\text{L}_2 = \text{C}_8\text{H}_8$), **6** ($\text{R} = \text{SiMe}_3$, $\text{L}_2 = \text{C}_8\text{H}_6(\text{SiMe}_3)_2$), **7** ($\text{R} = \text{H}$, $\text{L}_2 = \text{C}_8\text{H}_6(\text{SiMe}_3)_2$), **8** ($\text{R} = \text{H}$, $\text{L}_2 = \text{C}_6\text{H}_8$) and **9** ($\text{R} = \text{H}$, $\text{L}_2 = \text{C}_8\text{H}_{12}$)

$\eta^4\text{-C}_8\text{H}_6\text{R}'_2$					
Uncoord. CH	Coord. CH	$\mu_3\text{-C}_8\text{H}_6\text{R}_2$	SiMe_3	Other	
4	—	4.96 [4.02] ^a (s)	—	—	
5	6.11 [5.76] ^a (d, 4)	5.23 [5.39] ^a (dd, 4) ^b	4.94 [4.22] ^a (s, 8)	—	—
6	6.25(m, 2)	5.20(m, 2), 5.38(m, 2)	4.85(m, 2), 4.93(m, 4)	0.15(s, 18), 0.20(s, 18)	—
7	6.23(m, 2)	5.21(m, 2), 5.38(m, 2)	4.93(s, 8)	0.17(s, 18)	—
8	—	—	4.97 [4.26] ^a (s, 8)	—	1.86(m, 2), 2.23(m, 2), 5.00(m, 2), 6.20(m, 2) ^c [1.18(m, 2), 2.00(m, 2), 4.75(m, 2), 5.68(m, 2)] ^{a,c}
9	—	—	4.92 [4.28] ^a (s, 8)	—	2.6 [2.25] ^a (m, 8), 5.16 [5.34] ^a (s, 4) ^d

^a In C_6D_6 . ^b $J_{\text{RhH}} = 0.7$ Hz. ^c $\eta^4\text{-C}_6\text{H}_8$. ^d $\eta^4\text{-C}_8\text{H}_{12}$.

Table 3 ^{13}C NMR data [δ (multiplicity, J_{RhC} [Hz] where applicable), in CDCl_3] for $[\text{Rh}_4(\text{CO})_6(\mu_3\text{-C}_8\text{H}_6\text{R}_2)\text{L}_2]$ **4** ($\text{R} = \text{H}$, $\text{L} = \text{CO}$), **5** ($\text{R} = \text{H}$, $\text{L}_2 = \text{C}_8\text{H}_8$), **6** ($\text{R} = \text{SiMe}_3$, $\text{L}_2 = \text{C}_8\text{H}_6(\text{SiMe}_3)_2$), **7** ($\text{R} = \text{H}$, $\text{L}_2 = \text{C}_8\text{H}_6(\text{SiMe}_3)_2$), **8** ($\text{R} = \text{H}$, $\text{L}_2 = \text{C}_6\text{H}_8$) and **9** ($\text{R} = \text{H}$, $\text{L}_2 = \text{C}_8\text{H}_{12}$)

$\eta^4\text{-C}_8\text{H}_6\text{R}'_2$		$\mu_3\text{-C}_8\text{H}_6\text{R}_2$				
CO	C	CH	C	CH	SiMe_3	Other
4	^{a, b}	—	—	71.4	—	—
5	184.8(d, 98) ^b	—	92.2(d, 10), 135.0	71.2	—	—
6	186.5(d, 94), 227.2	151.7	94.6(d, 10), 97.6(d, 8), 144.2	72.7, 73.9, 74.4	−0.4, −1.0	—
7	185.5(d, 94), 226.9(dt, 34, 20)	151.7	94.8(d, 10), 96.8(d, 8), 144.1	71.1	−1.0	—
8	185.5(d, 94) ^b	—	—	70.8	—	25.2, 78.2(d, 12), 97.9(d, 6) ^c
9 ^d	186.9(d, 93), 228.0(m)	—	—	70.9(q, 1)	—	32.1, 91.7(d, 10) ^e

^a $\eta^1\text{-CO}$ not observed. ^b $\mu_3\text{-CO}$ not observed. ^c $\eta^4\text{-C}_6\text{H}_8$. ^d In C_6D_6 . ^e $\eta^4\text{-C}_8\text{H}_{12}$.

refined. The asymmetric unit of the crystal structure of **4** was found to contain four independent molecules, which are all quite similar. Two similar independent molecules are also present in the crystals of **8**. Views of the molecules are presented in Figs. 1–5. Relevant bond lengths are reported in Tables 4–7.

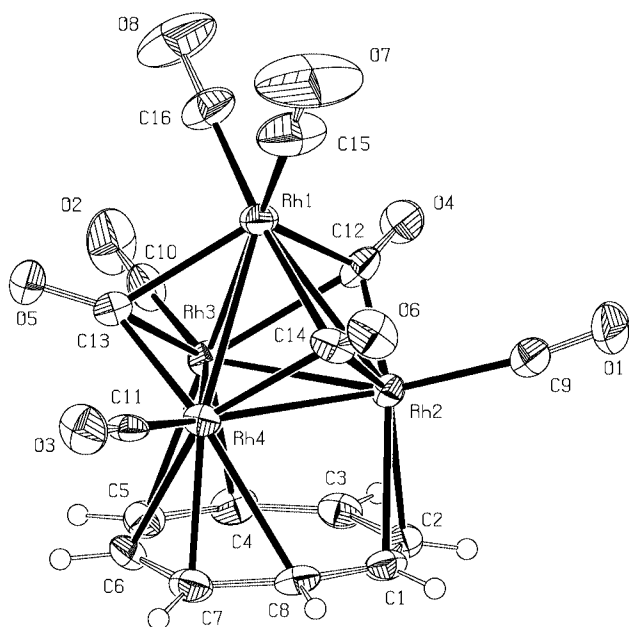


Fig. 1 Molecular structure of $[\text{Rh}_4(\text{CO})_8(\mu_3\text{-C}_8\text{H}_8)]$ **4**. Only one of the four crystallographically independent molecules is shown.

All the molecular structures consist of a pseudo-tetrahedral Rh_4 core, one face of which is capped by the facial $\text{C}_8\text{H}_6\text{R}_2$ ($\text{R} = \text{H}$, SiMe_3) ligand.¹³ The Rh_4 polyhedra are distorted from an ideal tetrahedral geometry. In all cases, the apical rhodium atom is displaced from a position above the centre of the basal Rh_3 plane, towards a basal apex or edge. This distortion causes the distances between the apical and the basal rhodium atoms

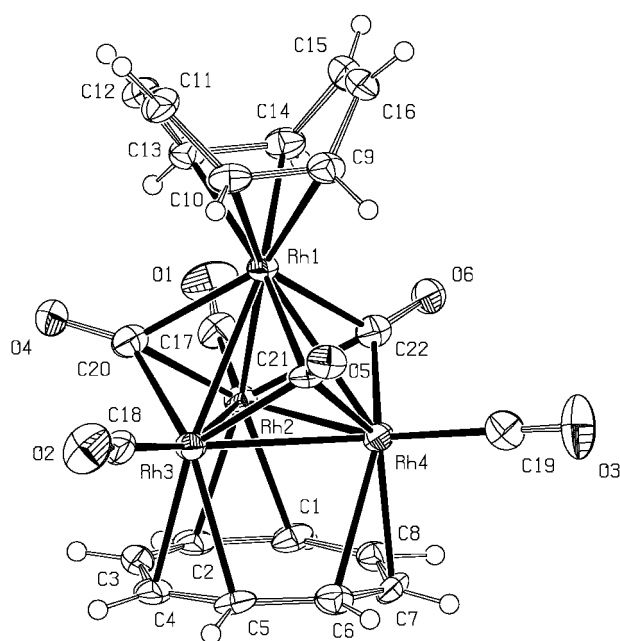


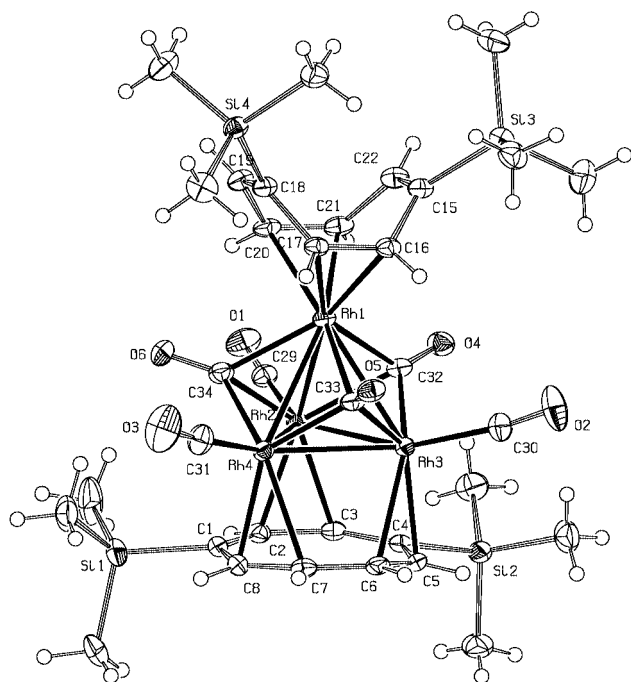
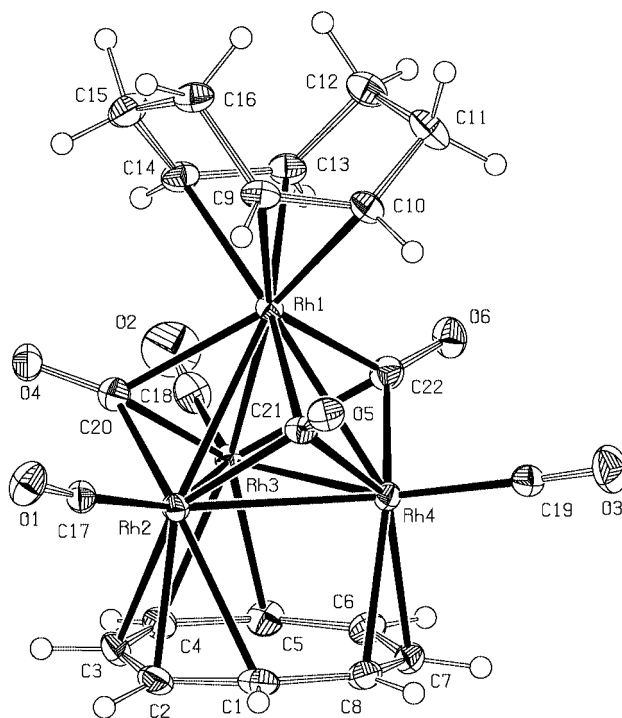
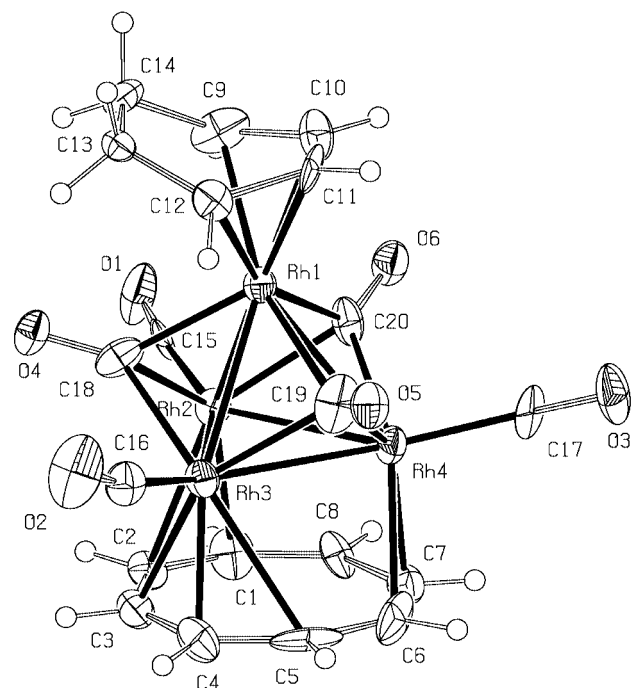
Fig. 2 Molecular structure of $[\text{Rh}_4(\text{CO})_6(\mu_3\text{-C}_8\text{H}_8)(\eta^4\text{-C}_8\text{H}_8)]$ **5**.

to vary considerably ($\Delta d = 0.10\text{--}0.27$ Å). With the exception of **8**, the metal–metal distances within the approximately equilateral basal Rh_3 triangle are slightly shorter than the $\text{Rh}_{\text{ap}}\text{--Rh}_{\text{bas}}$ bonds [mean values $d(\text{Rh}_{\text{bas}}\text{--Rh}_{\text{bas}})$: 2.74 Å (**4**), 2.74 Å (**5**), 2.73 Å (**6**), 2.74 Å (**9**); $d(\text{Rh}_{\text{ap}}\text{--Rh}_{\text{bas}})$: 2.76 Å (**4**), 2.78 Å (**5**), 2.77 Å (**6**), 2.77 Å (**9**)]. In the η^4 -cyclohexadiene complex **8**, the $\text{Rh}_{\text{bas}}\text{--Rh}_{\text{bas}}$ bonds are longer than the average $\text{Rh}_{\text{ap}}\text{--Rh}_{\text{bas}}$ distances (mean values 2.74 Å vs. 2.72 Å).

There are three terminal carbonyl ligands, one on every atom of the basal Rh_3 plane, bent away from the facial $\text{C}_8\text{H}_6\text{R}_2$ ligand towards the centre of the metal cluster. Three face-capping carbonyls occupy the remaining faces of the metal tetrahedron. The apical rhodium atom carries an η^4 -coordinated carbocycle (C_8H_8 in **5**, $\text{C}_8\text{H}_6(\text{SiMe}_3)_2$ in **6** and **7**, C_6H_8 in **8**, C_8H_{12} in **9**) or two terminal carbonyl ligands (in **4**). Coordination of the apical

Table 4 Selected bond lengths [\AA] for the complex $[\text{Rh}_4(\text{CO})_8(\mu_3\text{-C}_8\text{H}_8)]$ **4**

	Molecule A	Molecule B	Molecule C	Molecule D
$\text{Rh}_{\text{ap}}\text{--Rh}_{\text{bas}}$	2.644(1)–2.820(1) ^a	2.654(1)–2.920(1) ^a	2.652(1)–2.904(1) ^a	2.644(1)–2.863(1) ^a
	2.761[83] ^b	2.768[112] ^b	2.767[104] ^b	2.761[90] ^b
$\text{Rh}_{\text{bas}}\text{--Rh}_{\text{bas}}$	2.715(1)–2.752(1) ^a	2.730(1)–2.743(1) ^a	2.728(1)–2.745(1) ^a	2.726(1)–2.756(1) ^a
	2.739[17] ^b	2.737[5] ^b	2.734[8] ^b	2.740[12] ^b
$\text{Rh--C}(\mu\text{-cot})^a$	2.205(6)–2.724(7)	2.201(6)–2.596(6)	2.202(7)–2.567(7)	2.202(7)–2.579(7)
$\text{C--C}(\mu\text{-cot})^a$	1.403(9)–1.432(9)	1.400(9)–1.42(1)	1.38(1)–1.44(1)	1.40(1)–1.43(1)
$\text{Rh--C}(\text{O})_{\text{term}}^b$	1.908[12]	1.911[6]	1.898[11]	1.911[12]
$\text{Rh}_{\text{ap}}\text{--C}(\text{O})_{\text{br}}^a$	2.190(6)–2.353(6)	2.133(6)–2.386(6)	2.153(7)–2.378(7)	2.181(6)–2.344(6)
$\text{Rh}_{\text{bas}}\text{--C}(\text{O})_{\text{br}}^a$	2.024(6)–2.325(6)	2.014(7)–2.162(6)	2.016(6)–2.185(7)	2.040(7)–2.215(6)

^a Range of values. ^b Mean value with standard deviation of the mean in brackets.**Fig. 3** Molecular structure of $[\text{Rh}_4(\text{CO})_6\{\mu_3\text{-C}_8\text{H}_6(\text{SiMe}_3)_2\}\{\eta^4\text{-C}_8\text{H}_6(\text{SiMe}_3)_2\}]$ **6**.**Fig. 5** Molecular structure of $[\text{Rh}_4(\text{CO})_6(\mu_3\text{-C}_8\text{H}_8)(\eta^4\text{-C}_8\text{H}_{12})]$ **9**.**Fig. 4** Molecular structure of $[\text{Rh}_4(\text{CO})_6(\mu_3\text{-C}_8\text{H}_8)(\eta^4\text{-C}_6\text{H}_8)]$ **8**. Only one of the two crystallographically independent molecules is shown.

$\text{C}_8\text{H}_6\text{R}_2$ ligands in complexes **5–7** is in the 1,2,5,6- η^4 fashion through two non-adjacent carbon carbon double bonds. A tub conformation is adopted by these ligands. If present, the SiMe_3 groups are on the non-coordinated side of the apical cot ligand, directed away from the metal cluster.

The facial $\text{C}_8\text{H}_6\text{R}_2$ ligands are somewhat puckered, with the distinct tendency towards a chair conformation. The best planes through the ring carbons are essentially parallel to the Rh_3 coordination plane, consistently at a distance of 2.1 \AA .

The distances between the rhodium and the carbon atoms of the facial $\text{C}_8\text{H}_6\text{R}_2$ ligands cover the wide range of 2.15(2)–2.724(7) \AA . Carbon–carbon distances vary somewhat around the facial rings in a non-systematic manner (**4**: 1.403(9)–1.44(1) \AA ; **5**: 1.40(1)–1.43(1) \AA ; **6**: 1.411(4)–1.435(4) \AA ; **8**: 1.35(3)–1.47(3) \AA ; **9**: 1.405(5)–1.428(5) \AA). Endocyclic bond angles range from 131° to 138°.

The common packing motif of the molecular clusters **4**, **5** and **8** in the crystal lattice is a face-to-face interaction of the facial cyclooctatetraene rings. This leads to the formation of dimers, which interlock with their RhL_2 ends to form parallel chains. The crystals of complex **9** contain one molecule of toluene per asymmetric unit. Here, the cluster molecules are arranged in layers parallel to the ab crystal face. Within these layers all the molecules are aligned in the same direction. In the [001] direction, two such layers alternate with a layer comprised of toluene molecules (Fig. 6).

Table 5 Selected bond lengths [Å] for the complex $[\text{Rh}_4(\text{CO})_6(\mu_3\text{-C}_8\text{H}_8)(\eta^4\text{-C}_8\text{H}_8)]$ **5**

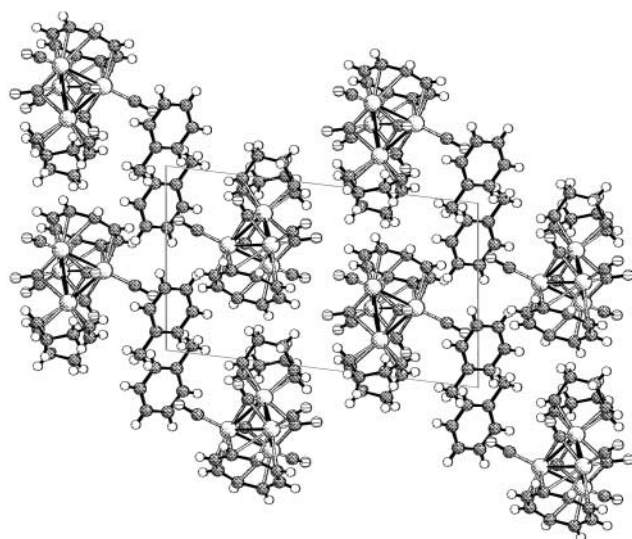
$\text{Rh}_{\text{ap}}\text{-Rh}_{\text{bas}}$	2.643(1)–2.887(2) ^a 2.777[100] ^b	$\text{Rh}_{\text{bas}}\text{-Rh}_{\text{bas}}$	2.7268(15)–2.752(2) ^a 2.741[10] ^b
$\text{Rh-C}(\mu\text{-cot})^a$	2.197(7)–2.711(8)	$\text{C-C}(\mu\text{-cot})^a$	1.40(1)–1.43(1)
$\text{Rh-C}(\eta^4\text{-cot})^a$	2.170(7)–2.194(8)		
$\text{Rh-C}(\text{O})_{\text{term}}^b$	1.906[5]	$\text{Rh}_{\text{ap}}\text{-C}(\text{O})_{\text{br}}^a$	2.168(8)–2.292(8)
$\text{Rh}_{\text{bas}}\text{-C}(\text{O})_{\text{br}}^a$	2.035(7)–2.290(8)		

^a Range of values. ^b Mean value with standard deviation of the mean in brackets.**Table 6** Selected bond lengths [Å] for the complex $[\text{Rh}_4(\text{CO})_6\{\mu_3\text{-C}_8\text{H}_6(\text{SiMe}_3)_2\}\{\eta^4\text{-C}_8\text{H}_6(\text{SiMe}_3)_2\}]$ **6**

$\text{Rh}_{\text{ap}}\text{-Rh}_{\text{bas}}$	2.6511(3)–2.8340(3) ^a 2.768[83] ^b	$\text{Rh}_{\text{bas}}\text{-Rh}_{\text{bas}}$	2.7133(3)–2.7564(3) ^a 2.734[18] ^b
$\text{Rh-C}(\mu\text{-cot})^a$	2.208(3)–2.660(4)	$\text{C-C}(\mu\text{-cot})^a$	1.411(4)–1.435(4)
$\text{Rh-C}(\eta^4\text{-cot})^a$	2.172(3)–2.212(3)		
$\text{Rh-C}(\text{O})_{\text{term}}^b$	1.902[8]	$\text{Rh}_{\text{ap}}\text{-C}(\text{O})_{\text{br}}^a$	2.191(3)–2.303(3)
$\text{Rh}_{\text{bas}}\text{-C}(\text{O})_{\text{br}}^a$	2.040(3)–2.184(3)		

^a Range of values. ^b Mean value with standard deviation of the mean in brackets.**Table 7** Selected bond lengths [Å] for the complexes $[\text{Rh}_4(\text{CO})_6(\mu_3\text{-C}_8\text{H}_8)(\eta^4\text{-C}_6\text{H}_8)]$ **8** and $[\text{Rh}_4(\text{CO})_6(\mu_3\text{-C}_8\text{H}_8)(\eta^4\text{-C}_8\text{H}_{12})]$ **9**

	8		9
	Molecule A	Molecule B	
$\text{Rh}_{\text{ap}}\text{-Rh}_{\text{bas}}$	2.684(4)–2.789(4) ^a 2.724[47] ^b	2.682(4)–2.800(4) ^a 2.723[55] ^b	2.6524(3)–2.8657(3) ^a 2.765[88] ^b
$\text{Rh}_{\text{bas}}\text{-Rh}_{\text{bas}}$	2.719(4)–2.758(4) ^a 2.743[17] ^b	2.738(4)–2.749(4) ^a 2.745[5] ^b	2.7221(3)–2.7502(3) ^a 2.738[12] ^b
$\text{Rh-C}(\mu\text{-cot})^a$	2.15(2)–2.68(3)	2.17(2)–2.69(3)	2.199(3)–2.689(3)
$\text{C-C}(\mu\text{-cot})^a$	1.38(3)–1.44(3)	1.35(3)–1.47(3)	1.405(5)–1.428(5)
$\text{Rh-C}(\text{C}_6\text{H}_8)^a$	2.09(2)–2.22(2)	2.13(2)–2.21(2)	
$\text{Rh-C}(\text{C}_8\text{H}_{12})^a$			2.187(3)–2.223(3)
$\text{Rh-C}(\text{O})_{\text{term}}^b$	1.874[18]	1.895[18]	1.900[9]
$\text{Rh}_{\text{ap}}\text{-C}(\text{O})_{\text{br}}^a$	2.12(2)–2.22(2)	2.10(2)–2.21(2)	2.113(3)–2.275(3)
$\text{Rh}_{\text{bas}}\text{-C}(\text{O})_{\text{br}}^a$	2.06(2)–2.14(2)	2.06(2)–2.17(2)	2.034(3)–2.302(3)

^a Range of values. ^b Mean value with standard deviation of the mean in brackets.**Fig. 6** Packing diagram of crystalline $[\text{Rh}_4(\text{CO})_6(\mu_3\text{-C}_8\text{H}_8)(\eta^4\text{-C}_8\text{H}_{12})]\cdot\text{C}_7\text{H}_8$.

The packing of the cluster molecules in crystalline **6** is quite different. Here, each of the forks formed by the two trimethylsilyl groups that are sticking out of both ends of one molecule points into the less restricted space around the 'waist' of another, to give a criss-cross arrangement. The overall efficiency of the packing is still less in this case, with only 65% space fill as compared to about 73% for crystalline **4** and **5**.

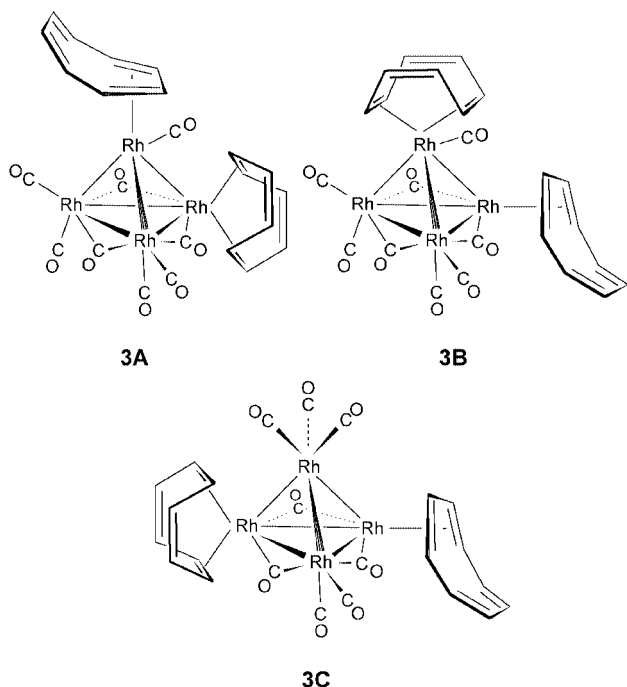
Discussion

(a) Syntheses and spectroscopic properties

In our earlier paper on the synthesis of $[\text{Co}_4(\text{CO})_6(\mu_3\text{-C}_8\text{H}_8)(\eta^4\text{-C}_8\text{H}_8)]$ **1** from $[\text{Co}_4(\text{CO})_{12}]$ and cot the question was raised whether this complex was formed *via* a mono-cot intermediate with an apical or with a facial cot ligand.⁹ Whilst this issue still remains unresolved in the cobalt case, our results with $[\text{Rh}_4(\text{CO})_{12}]$ **2** and cot clearly show that formation of $[\text{Rh}_4(\text{CO})_8(\mu_3\text{-C}_8\text{H}_8)]$ **4** precedes the substitution of two further carbonyl ligands, to form the facial/apical bis-cot complex $[\text{Rh}_4(\text{CO})_6(\mu_3\text{-C}_8\text{H}_8)(\eta^4\text{-C}_8\text{H}_8)]$ **5**. Apparently, formation of **5** from **4** requires considerably more energy than generation of the latter from the binary carbonyl. Hence, only **4** is formed selectively at low temperature. The low solubility of **4** and **5** in aliphatic hydrocarbon solvents is also likely to have some effect, removing **4** from the solution and thus impeding further reaction. Accordingly, with the disubstituted cyclooctatetraene, which greatly improves solubility, reaction of **2** immediately proceeds to give the facial/apical disubstituted cluster complex $[\text{Rh}_4(\text{CO})_6\{\mu_3\text{-C}_8\text{H}_6(\text{SiMe}_3)_2\}\{\eta^4\text{-C}_8\text{H}_6(\text{SiMe}_3)_2\}]$ **6**, even at low temperature.

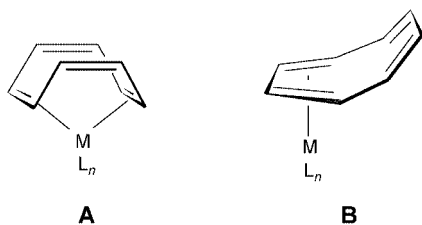
The properties of the hexacarbonyl complex **5** are essentially identical to those reported earlier⁸ for the material which had been obtained from **2** and cot in benzene. The composition $[\text{Rh}_4(\text{CO})_8(\eta^4\text{-C}_8\text{H}_8)_2]$ **3** was assigned to this product based on elemental analysis and a molecular weight measurement. To account for the ¹H NMR spectrum, three possible structures **3A–3C** were suggested, each with a fluxional 1,2,3,4- $\eta^4\text{-C}_8\text{H}_8$ and a non-fluxional 1,2,5,6- $\eta^4\text{-C}_8\text{H}_8$ ligand. We propose that

the complex in question really was the hexacarbonyl **5**. In an octacarbonyl **3** there is an obvious steric problem to simultaneously accommodate two cot ligands and eight carbonyls in the coordination shell of the Rh₄ tetrahedron. Moreover, as illustrated by the facile formation of **4**, on the Rh₄ frame apical cot is highly unlikely to be stable with respect to rearrangement into the facial coordination.



As in [Co₄(CO)_{8-2n}(μ₃-C₈H₈)(η⁴-C₈H₈)_n] **10** (*n* = 0)⁹ and **1** (*n* = 1)⁹, only the apical ligands (CO and cot, respectively) in complexes **4** and **5** are prone to substitution. This again demonstrates the high kinetic and thermodynamic stability of the facial coordination mode for cyclooctatetraene and its derivatives. The IR (ν_{CO}) and NMR spectroscopic properties of the tetrahetero cluster complexes **4–9** are quite straightforward and parallel those of their tetracobalt analogues. The observation of temperature independent singlet resonances for the facial cot ligands in the ¹H and ¹³C NMR spectra, respectively, is indicative of very small barriers for rotation of this ligand within its coordination plane on the Rh₄ cluster. The proton resonances are at somewhat lower field than those of the tetracobalt analogues. The observed strong dependence of the proton chemical shifts on the solvent parallels the behaviour of the cobalt complexes.

The geometric preferences of tetrahapto-bonded cot have received considerable attention.¹⁴ Two common coordination geometries prevail: 1,2,5,6-η⁴-bonding of the cyclopolyene through non-adjacent double bonds as a chelating 1,5-diene system (**A**), and 1,2,3,4-η⁴-bonding as a conjugated 1,3-diene (**B**).



The electronic factors which govern the favoured mode of bonding have not been identified with confidence.¹⁵ In only one system, namely [(η-C₅R₅)Co(C₈H₈)] **11a** (R = H),¹⁶ **11b** (R = Me),¹⁷ has a measurable equilibrium between the two isomers been identified in solution. In the crystalline solid, **11a** has the

1,2,5,6-η⁴-ligand,¹⁸ this is also the more abundant isomer in solution. The 1,2,5,6-η⁴ structure is also thermodynamically preferred for [(η-C₅Me₅)Rh(C₈H₈)]. The 1,2,3,4-η⁴-isomer is formed as a transient kinetic product if and only if this complex is prepared below –20 °C.¹⁹

Independent on the temperature, the apical cot ligand in **5** gives two resonances each in the proton and carbon spectra, in contrast to **1**, where only one resonance is observed. This is clearly indicative of this ligand adopting the non-fluxional 1,2,5,6-η⁴-coordination mode, in contrast to the highly dynamic 1,2,3,4-η⁴-coordination found in **1**. More possibilities exist for the η⁴-coordination of 1,4-C₈H₆(SiMe₃)₂. In the free state, this ligand exists in the form of an equilibrium mixture of the two double bond shifted isomers 1,4-(SiMe₃)₂-1,3,5,7-C₈H₆ **C** and 1,4-(SiMe₃)₂-2,4,6,8-C₈H₆ **D** (Chart 1).^{20,21} No quantitative

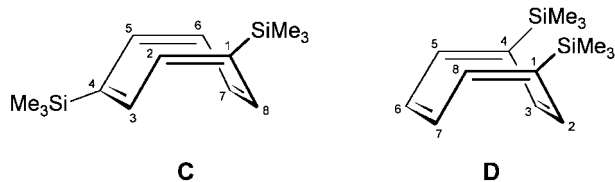


Chart 1

experimental data are available with respect to the energy difference between the two isomers and the activation barrier for their interconversion. The arrangements resulting from 1,5-diene- and 1,3-diene-like coordination to a metal of these isomers are depicted schematically in Chart 2. Structure 1,3-**D**(2) has been found in the mononuclear complex [(η⁸-C₈H₆(SiMe₃)₂)Hf{η⁸-C₈H₆(SiMe₃)₂}].²² The corresponding titanium complex shows a similar arrangement, but with a tendency towards an η³-coordination mode.²³

For complex **6**, the observed number of resonances due to the apical C₈H₆(SiMe₃)₂ ligand in the proton and carbon NMR spectra immediately rules out the less symmetric possibilities 1,5-**C**, 1,3-**C**(3), 1,3-**D**(1) and 1,3-**D**(2). Of the remaining four structures only 1,5-**D**(1) is also compatible with the observed chemical shifts and the couplings to the ¹⁰³Rh nucleus (Tables 2 and 3). Clearly, a nominal 2,3,6,7-η⁴-coordination is attained by the apical ligand in solution. On steric grounds, this is the more favourable one of the two 1,5-**D** structures, with the bulky trimethylsilyl groups pointing away from the metal cluster. The complexes **6** and **7** were obtained in high yields. We therefore have to assume that rearrangement of the ligand isomer **C** into **D** occurs during the reaction.

Chemical shifts in the range δ = 70–80 have been reported for the rhodium coordinated carbons in 1,2,5,6-η⁴-cot.^{19,24} The corresponding values are about 20 ppm higher in **5–7**, and are otherwise only matched by cationic cot complexes.²⁴ The carbon resonances of the carbonyl ligands indicate a lack of fluxionality of the Rh₄(μ₃-CO)₃(η¹-CO)₃ moiety on the NMR time scale. The observed number of resonances and their coupling pattern (coupling to three ¹⁰³Rh, two of which are equivalent, for the face-capping carbonyls; coupling to one ¹⁰³Rh for the terminal carbonyls) rules out exchange between the μ₃ and η¹ sites, as well as exchange processes involving only the terminal or bridging carbonyl ligands.

Molecular structures

The molecular structures of the complexes [Rh₄(CO)₆(μ₃-C₈H₆R₂)L₂] **4** (R = H, L = CO), **5** (R = H, L₂ = η⁴-C₈H₈), **6** (R = SiMe₃, L₂ = η⁴-C₈H₆(SiMe₃)₂), **7** (R = H, L₂ = η⁴-C₈H₆(SiMe₃)₂), **8** (R = H, L₂ = η⁴-C₆H₈) and **9** (R = H, L₂ = η⁴-C₈H₁₂) follow the general pattern that has been established previously for numerous cluster complexes of the type [Co₄(CO)₆(μ₃-C₈H₈-L₂)]^{1,9,11} This also includes the less prominent geometric features, like the above-mentioned variations of the M_{ap}–M_{bas}

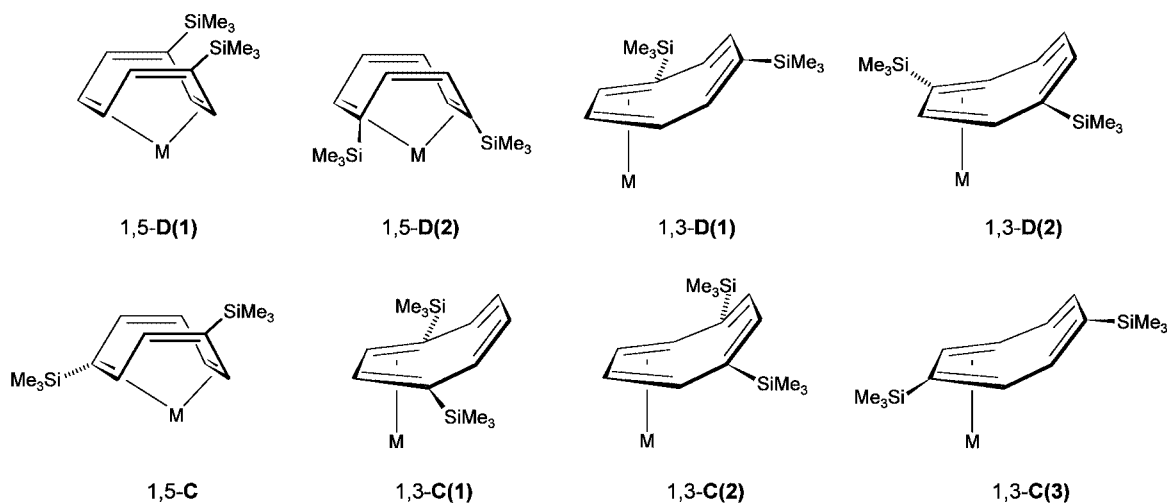


Chart 2

distances, which are common to the cobalt and the rhodium series. The coordination geometries of the facial C_8H_8 ligands in the Co_3 and Rh_3 coordination sites are also very similar. With respect to the coordination geometry, folding and the distribution of endocyclic bond lengths and angles, the bulky trimethylsilyl groups do not have much influence on the facial cyclooctatetraene ligand.

The structural evidence that has become available in recent years now allows a few more general statements on facial coordination of the conjugated π -perimeters C_nH_n ($n = 6-8$). In the large class of cluster complexes with a $M_3(\mu_3\text{-arene})$ ($n = 6$) structural motif, the sixfold symmetry of the facial ligand is compatible with the local threefold symmetry of the trimetal coordination site [the local C_{3v} symmetry of the coordination site constitutes a subgroup of the point group of the free ligand (ideally D_{6h})]. This match of symmetry, which has a direct influence on metal-to-ligand bonding, in the overwhelming majority of cases favours the staggered coplanar arrangement of the M_3 and C_6 rings, corresponding to the well known $\mu_3\text{-}\eta^2 : \eta^2 : \eta^2$ coordination geometry. A certain degree of double bond localisation is characteristic for $\mu_3\text{-}\eta^2 : \eta^2 : \eta^2$ -coordinated arenes, with a corresponding usually slight but distinct alternation of longer and shorter endocyclic carbon carbon bonds.²⁵ The potential energy well is deep enough to generate barriers for in-plane rotation of the μ_3 -arene which correspond to activation enthalpies of some 50 kJ mol^{-1} .²⁶

However, the eightfold symmetry of a (planar) cyclooctatetraene does not match that of the M_3 coordination site. For this reason, there are many nominally different orientations of the eight membered ring on top of the metal triangle, which are however geometrically quite similar and do not differ much in energy.¹ As a consequence, the intrinsic barriers to in-plane rotation are much smaller, and a quasi continuous range of coordination modes between $\eta^2 : \eta^3 : \eta^3$ and $\eta^3 : \eta^3 : \eta^3$ is attainable. It should be noted here that in the crystalline solids facial cot ligands normally occupy well defined positions, *i.e.* rotational disorder is not observed. However, such complexes very frequently crystallize with several molecules in the asymmetric unit, which mainly differ in the orientations of the facial cyclooctatetraene ligands. This is an indication of rotational energy barriers in the crystals being determined by intermolecular forces, such as hydrogen bonding and interlocking of the CH bonds.⁹ In most of the complexes discussed here one of the carbon atoms of the facial cyclooctatetraene is quite far away from the nearest rhodium atom, 2.660(4) Å (in **6**) to 2.724(7) Å (in one molecule of **4**), on the verge or even beyond a bonding interaction. It has, however, to be noted that the chair-like folding of the ring tends to minimize the longest rhodium carbon distances. Similar situations are encountered in the complexes $[Co_4(CO)_6(\mu_3\text{-}C_8H_8)L_2]$ ($L = CO, L_2 = C_8H_8, C_6H_6$)⁹

and in $[Ru_3(CO)_5\{\mu_3\text{-}P(Ph)CH_2PPh_2\}(\mu_3\text{-}C_8H_8)(Ph)]$.²⁷ As has been noticed before, not too much significance should be attached to the solid state structures in this respect, due to the very high fluxionality of the facial cyclooctatetraenes.

In contrast to $[Co_4(CO)_6(\mu_3\text{-}C_8H_8)(1\text{-}4\text{-}\eta\text{-}C_8H_8)]$ **1** the apical $C_8H_6R_2$ ligands ($R = H, SiMe_3$) in **5**, **6** and **7** adopt the 1,2,5,6- η^4 -coordination mode, *via* two non-adjacent double bonds. In the crystals of complex **6**, the apical $C_8H_6(SiMe_3)_2$ is the 1,4-($SiMe_3$)₂-2,4,6,8-tetraene isomer (**1,5-D(1)** in Chart 2), in agreement with the spectroscopic data in solution (*vide supra*). This ligand system has not been described previously. The tub conformations adopted by the apical C_8H_8 ligands are less 'open' in the complexes than in the free cyclopolyolefins. Fold angles along the transannular vectors connecting the metal bound ring carbons C9 with C14 and C10 with C13 are 125° and 127° in **5**, compared to 126° in the mononuclear cobalt complex **11a** and 138° in crystalline C_8H_8 .²⁸ respectively. The corresponding fold angles in $\eta^4\text{-}C_8H_6(SiMe_3)_2$ are larger (135° and 136°), probably due to repulsion of the $SiMe_3$ groups. The structures of the two isomers of free 1,4- $C_8H_6(SiMe_3)_2$ are unknown. Optimization of this molecule with *ab initio* DFT methods converges to the two minima 1,4-($SiMe_3$)₂-1,3,5,7-tetraene (**C** in Chart 1) and 1,4-($SiMe_3$)₂-2,4,6,8-tetraene (**D** in Chart 1), with very little energy difference between these two tub-shaped isomers.²⁹

In the molecules of **5**, **6**, **7** and **9** one of the metal coordinated carbon-carbon bonds of the apical cyclooctatetraene or cyclooctadiene ligand (*e.g.* C13-C14 in **5**, Fig. 2) is perpendicular to the shortest $Rh_{ap}\text{-}Rh_{bas}$ bond of the respective metal cluster, approximately *trans* to a rhodium-rhodium bond within the basal Rh_3 face. This arrangement places the facial carbonyl ligand associated with this $Rh_{bas}\text{-}Rh_{bas}$ bond (*e.g.* C21-O5 in **5**) in the proximity of the second coordinated carbon-carbon bond of the η^4 -cyclooctatetraene (*e.g.* C9-C10 in **5**). Steric hindrance is minimized by a tilt of the apical ligand, which places the η^4 coordination plane at an angle (8° in **5** and 6, 7° in **9**) to the basal Rh_3 plane.

Crystal packing

The packing of the cluster molecules $[Co_4(CO)_6(\mu_3\text{-}C_8H_8)L_2]$ **1** ($L_2 = C_8H_8$), **10** ($L = CO$) and **12** ($L_2 = C_6H_6$) to form the crystal lattice has been examined in detail.⁹ These structures support the general idea that the packing of transition metal clusters possessing both flat cyclopolyene and tubular carbonyl ligands is best coped with by packing together the fragments with similar shape. The crystal structures of their tetrarhodium analogues **5**, **4** and **8** closely follow the same pattern.

The crystal structures of **8** and **12** are isomorphous, with two independent molecules in the asymmetric unit, which in both

cases only differ in the rotational orientation of their μ_3 -C₈H₈ ligands with respect to the M₃ coordination plane. The lattice of the rhodium complex **4** has a lower symmetry (four independent molecules in space group $P2_1/n$, which is an alternative setting of $P2_1/c$) than its cobalt counterpart **10** (two independent molecules in space group $C2/c$). The arrangement of the molecules is however still essentially the same in both structures. The translational symmetry element that makes up the C centering is only approximate in the structure of **4**, due to a slight twist of the cluster molecules.

Conclusion

Our results presented in this paper clearly illustrate the distinct preference of cyclooctatetraene for the facial coordination on a tetrahedral Rh₄ frame. At least for the tetrarhodium systems, facial (μ_3) coordination is much preferred to an apical coordination site. When the complex [Rh₄(CO)₈(μ_3 -C₈H₈)] **4** is formed from [Rh₄(CO)₁₂] **2** and cot, three of the carbonyl ligands on the coordinating basal Rh₃ face are displaced, to account for six of the eight electrons donated by the facial C₈H₈ ligand. The fourth electron pair can be accommodated within the cluster after loss of another CO from the apical metal atom, which does not directly participate in bonding the cyclic hydrocarbon. Hence, all four metal atoms of the cluster are effectively involved in the formation of the M₃(μ_3 -C₈H₈) moiety, a nice example of cooperative multi-metal reactivity.

Experimental

General procedures

All operations were carried out under an atmosphere of purified nitrogen or argon (BASF R3-11 catalyst) using Schlenk techniques. Solvents were dried by conventional methods. NMR spectra were obtained on Bruker AC 200 and AVANCE DRX200 instruments (200.1 MHz for ¹H, 50.3 MHz for ¹³C). ¹H and ¹³C chemical shifts are reported vs. SiMe₄ and were determined by reference to internal SiMe₄ or residual solvent peaks. Assignment of the carbon resonances was routinely augmented by ¹³C-¹H DEPT (135°) spectra. Infrared spectra were recorded in CaF₂ cells with a Bruker IFS-28 Fourier transform spectrometer (optical resolution 0.5 cm⁻¹). Elemental analyses were performed locally by the microanalytical laboratory of the Organisch-chemisches Institut der Universität Heidelberg and by Mikroanalytisches Labor Beller, Göttingen.

Syntheses

[Rh₄(CO)₈(μ_3 -C₈H₈)] **4**. (a) From [Rh₄(CO)₁₂] **2** and cot. A mixture of 900 mg (1.2 mmol) of **2** and 0.5 ml (4.3 mmol) of cot in 200 ml of *n*-pentane was heated to gentle reflux. The course of the reaction was monitored by IR spectroscopy. The mixture was cooled to room temperature when the absorptions of **2** were no longer detectable. The black precipitate was collected on a fine frit and washed several times with *n*-pentane. Recrystallization from CH₂Cl₂ gave 865 mg (98% yield) of black crystalline [Rh₄(CO)₈(μ_3 -C₈H₈)] **4**.

(b) From [Rh₄(CO)₆(μ_3 -C₈H₈)(η^4 -C₈H₈)] **5** and [Fe(CO)₅]. A toluene solution (120 ml) of **5** (140 mg, 0.2 mmol) and [Fe(CO)₅] (0.5 ml, 3.7 mmol) was heated to 70 °C for 3 h. The mixture was cooled to ambient temperature and filtered. Removal of the solvent under reduced pressure gave **4** as a black residue which was washed several times with *n*-pentane. Yield 80 mg (60%). FD-MS (*m/z*, rel. int. [%]): 739.5 (100, M⁺). Anal. (%) calc. for C₁₆H₈O₈Rh₄: C 25.98, H 1.09; found C 25.95, H 1.33.

[Rh₄(CO)₆(μ_3 -C₈H₈)(η^4 -C₈H₈)] **5**. (a) From [Rh₄(CO)₁₂] **2** and cot. A mixture of 3.20 g (4.3 mmol) of **2** and 2.0 ml

(17.3 mmol) of cot in 200 ml of *n*-heptane was heated to reflux. The course of the reaction was monitored by IR spectroscopy. The mixture was cooled to room temperature as soon as the absorptions of **2** were no longer detectable (*ca.* 5 h). The black precipitate was collected on a fine frit, washed several times with *n*-pentane and then extracted with CH₂Cl₂. Solvent was removed from the extract under reduced pressure and the black residue was recrystallized from CH₂Cl₂ to give 3.25 g (96% yield) of black crystalline [Rh₄(CO)₆(μ_3 -C₈H₈)(η^4 -C₈H₈)] **5**. FD-MS (*m/z*, rel. int. [%]): 787.6 (100, M⁺). Anal. (%) calc. for C₂₂H₁₆O₆Rh₄: C 33.53, H 2.05; found C 33.64, H 2.34.

(b) From [Rh₄(CO)₈(μ_3 -C₈H₈)] **4** and cot. A mixture of 250 mg (0.34 mmol) of **4** and 0.2 ml (1.7 mmol) of cot in 100 ml of toluene was heated to reflux for 6 h. The mixture was cooled to room temperature and filtered. Solvent was removed from the filtrate under reduced pressure to give 255 mg (95% yield) of black [Rh₄(CO)₆(μ_3 -C₈H₈)(η^4 -C₈H₈)] **5**.

[Rh₄(CO)₆(μ_3 -C₈H₆(SiMe₃)₂)(η^4 -C₈H₆(SiMe₃)₂)] **6**. A mixture of 500 mg (0.6 mmol) of **2** and 340 mg (1.3 mmol) of 1,4-(SiMe₃)₂C₈H₆ in 150 ml of *n*-pentane was heated to reflux. The course of the reaction was monitored by IR spectroscopy. The mixture was cooled to room temperature when the absorptions of **2** were no longer detectable (*ca.* 3 h). A small amount of a black precipitate was removed by filtration. Solvent was removed from the filtrate under reduced pressure to give a dark residue which was recrystallized from *n*-pentane. Yield: 675 mg (99%) of dark red microcrystalline [Rh₄(CO)₆(μ_3 -C₈H₆(SiMe₃)₂)(η^4 -C₈H₆(SiMe₃)₂)] **6**. FD-MS (*m/z*, rel. int. [%]): 1076.0 (100, M⁺). Anal. (%) calc. for C₃₄H₄₈O₆Rh₄Si₄: C 37.93, H 4.49; found C 37.76, H 4.61.

[Rh₄(CO)₆(μ_3 -C₈H₈)(η^4 -C₈H₆(SiMe₃)₂)] **7**. A mixture of 140 mg (0.20 mmol) of **4** and 50 mg (0.20 mmol) of 1,4-(SiMe₃)₂C₈H₆ in 200 ml of *n*-heptane was heated to reflux. The course of the reaction was monitored by IR spectroscopy. The mixture was cooled to room temperature when the absorptions of **4** were no longer detectable (*ca.* 2 h). A small amount of a black precipitate was removed by filtration. Solvent was removed from the filtrate under reduced pressure to give a dark residue which was recrystallized from *n*-pentane. Yield: 180 mg (98%) of deep red microcrystalline [Rh₄(CO)₆(μ_3 -C₈H₈)(η^4 -C₈H₆(SiMe₃)₂)] **7**. FD-MS (*m/z*, rel. int. [%]): 932.0 (100, M⁺). Anal. (%) calc. for C₂₈H₃₂O₆Rh₄Si₂: C 36.07, H 3.46; found C 36.07, H 3.95.

[Rh₄(CO)₆(μ_3 -C₈H₈)(η^4 -C₆H₈)] **8**. A mixture of 350 mg (0.45 mmol) of **5** and 0.5 ml (5.2 mmol) of 1,3-cyclohexadiene in 100 ml of toluene was heated to reflux for 2.5 h. After cooling of the solution to room temperature a small amount of black precipitate was removed by filtration. All volatiles were removed from the filtrate under reduced pressure and the residue was recrystallized from toluene to give 255 mg (75% yield) of red-brown crystalline [Rh₄(CO)₆(μ_3 -C₈H₈)(η^4 -C₆H₈)] **8**. FD-MS (*m/z*, rel. int. [%]): 763.3 (100, M⁺). Anal. (%) calc. for C₂₀H₁₆O₆Rh₄: C 31.44, H 2.11; found C 31.81, H 2.59.

[Rh₄(CO)₆(μ_3 -C₈H₈)(η^4 -C₈H₁₂)] **9**. A mixture of 280 mg (0.36 mmol) of **5** and 0.45 ml (3.5 mmol) of 1,5-cyclooctadiene in 100 ml of toluene was heated under reflux for 3 h. After cooling of the solution to room temperature a small amount of black precipitate was removed by filtration. All volatiles were removed from the filtrate under reduced pressure and the residue was recrystallized from toluene to give 200 mg (70% yield) of brown crystalline [Rh₄(CO)₆(μ_3 -C₈H₈)(η^4 -C₈H₁₂)] **9**. FD-MS (*m/z*, rel. int. [%]): 792.0 (100, M⁺); HR-MS (FAB⁺): calc. for C₂₂H₂₀O₆Rh₄ 791.7480, found 791.7432.

Crystal structure determinations

Single crystals were grown from methylene chloride (**4**–**6**) or

toluene solutions at 2–8 °C (**8**, **9**). Crystal data are compiled in Tables 8 and 9. Intensity data were collected at low temperature on a Siemens-Stoe AED2 four circle diffractometer and on a Bruker AXS SMART CCD diffractometer. A semi-empirical absorption correction was applied. The structures were solved by direct methods, and refined by full matrix least squares based on F^2 using all measured unique reflections. All non-hydrogen atoms were given anisotropic displacement parameters. For complexes **4**, **5**, **6** and **9** all hydrogen atoms were located from difference Fourier syntheses and refined with isotropic displacement parameters (except for one methyl substituent in **6**, which was treated as a rigid group). All hydrogens of complex **8** were input in calculated positions.

A limited set of reflection data was also collected from a poorly crystalline specimen of $[\text{Rh}_4(\text{CO})_6(\mu_3\text{-C}_8\text{H}_8)\{\eta^4\text{-C}_8\text{H}_6(\text{SiMe}_3)_2\}]$ **7**. The low quality of this dataset allowed the structure to be solved, but was not sufficient for a complete refinement. The calculations were performed using the programs SHELXS-86 and SHELXL-97.³⁰ Graphical representations were drawn with PLATON³¹ and SCHAKAL-99.³² Anisotropic displacement ellipsoids are scaled to 40% probability.

Table 8 Details of the crystal structure determinations of $[\text{Rh}_4(\text{CO})_6(\mu_3\text{-C}_8\text{H}_8)]$ **4** and $[\text{Rh}_4(\text{CO})_6(\mu_3\text{-C}_8\text{H}_8)(\eta^4\text{-C}_8\text{H}_8)]$ **5**

	4	5
Formula	$\text{C}_{16}\text{H}_8\text{O}_8\text{Rh}_4$	$\text{C}_{22}\text{H}_{16}\text{O}_6\text{Rh}_4$
M_r	739.86	787.99
Crystal system	Monoclinic	Triclinic
Space group	$P2_1/n$	$P\bar{1}$
T/K	203(2)	203(2)
$a/\text{\AA}$	22.209(11)	8.889(5)
$b/\text{\AA}$	13.520(7)	9.195(7)
$c/\text{\AA}$	25.495(13)	13.700(7)
$\alpha/^\circ$	90	81.04(3)
$\beta/^\circ$	102.79(4)	78.70(3)
$\gamma/^\circ$	90	74.22(3)
$V/\text{\AA}^3$	7465(7)	1050.4(9)
Z	16	2
$\mu(\text{Mo-K}\alpha)/\text{mm}^{-1}$	3.52	3.13
Reflections measured	13126	3689
Unique	13126	3689
Observed [$I > 2\sigma(I)$]	11108	2944
R -values		
R (obs. reflections)	0.032	0.036
$wR2$ (all reflections)	0.083	0.088

Table 9 Details of the crystal structure determinations of $[\text{Rh}_4(\text{CO})_6\{\mu_3\text{-C}_8\text{H}_6(\text{SiMe}_3)_2\}\{\eta^4\text{-C}_8\text{H}_6(\text{SiMe}_3)_2\}]$ **6**, $[\text{Rh}_4(\text{CO})_6(\mu_3\text{-C}_8\text{H}_8)(\eta^4\text{-C}_8\text{H}_6)]$ **8** and $[\text{Rh}_4(\text{CO})_6(\mu_3\text{-C}_8\text{H}_8)(\eta^4\text{-C}_8\text{H}_{12})]$ **9**

	6	8	9-C₇H₈
Formula	$\text{C}_{34}\text{H}_{48}\text{O}_6\text{Rh}_4\text{Si}_4$	$\text{C}_{20}\text{H}_{16}\text{O}_6\text{Rh}_4$	$\text{C}_{22}\text{H}_{20}\text{O}_6\text{Rh}_4\text{-C}_7\text{H}_8$
M_r	1076.72	763.97	884.15
Crystal system	Monoclinic	Triclinic	Triclinic
Space group	$P2_1/n$	$P\bar{1}$	$P\bar{1}$
T/K	173(2)	203(2)	190(2)
$a/\text{\AA}$	12.3544(2)	10.195(10)	8.2841(4)
$b/\text{\AA}$	16.8339(3)	11.249(13)	10.4702(5)
$c/\text{\AA}$	20.2878(3)	18.16(2)	17.0483(8)
$\alpha/^\circ$	90	81.40(9)	80.431(1)
$\beta/^\circ$	93.051(1)	85.42(9)	80.432(1)
$\gamma/^\circ$	90	81.04(9)	70.294(1)
$V/\text{\AA}^3$	4213.3(1)	2031(4)	1363.0(1)
Z	4	4	2
$\mu(\text{Mo-K}\alpha)/\text{mm}^{-1}$	1.69	3.23	2.42
Reflections measured	41388	4822	24178
Unique, R_{int}	10272, 0.041	4822	9077, 0.042
Observed [$I > 2\sigma(I)$]	9141	3031	7074
R -values			
R (obs. reflections only)	0.028	0.063	0.031
$wR2$ (all reflections)	0.068	0.163	0.069

CCDC reference numbers 166159–166163.

See <http://www.rsc.org/suppdata/dt/b1/b105485f/> for crystallographic data in CIF or other electronic format.

Acknowledgements

This work was supported by the Sonderforschungsbereich 247 der Universität Heidelberg and the Fonds der Chemischen Industrie. Donations of valuable chemicals by BASF AG Ludwigshafen and DEGUSSA AG Hanau are gratefully acknowledged.

References and notes

- H. Wadepohl, *Coord. Chem. Rev.*, 1999, **185–186**, 551.
- E. O. Fischer, O. S. Mills, E. F. Paulus and H. Wawersik, *Chem. Commun.*, 1967, 643; O. S. Mills and E. F. Paulus, *J. Organomet. Chem.*, 1968, **11**, 587.
- (a) M. D. Brice, R. J. Dellaca, B. R. Penfold and J. L. Spencer, *J. Chem. Soc. D*, 1971, 72; (b) R. J. Dellaca and B. R. Penfold, *Inorg. Chem.*, 1972, **11**, 1855.
- G. A. Somorjai and U. Starke, *Pure Appl. Chem.*, 1992, **64**, 509.
- (a) G. A. Somorjai, *J. Phys. Chem.*, 1990, **94**, 1013; (b) F. P. Netzer, *Langmuir*, 1991, **7**, 2544; (c) F. P. Netzer and M. G. Ramsey, *Crit. Rev. Solid State Mater. Sci.*, 1992, **17**, 397.
- (a) M. A. van Hove, R. F. Lin and G. A. Somorjai, *Phys. Rev. Lett.*, 1983, **51**, 778; R. F. Lin, G. S. Blackman, M. A. van Hove and G. A. Somorjai, *Acta Crystallogr., Sect. B*, 1987, **43**, 368; (b) M. Neumann, J. U. Mack, E. Bertel and F. P. Netzer, *Surf. Sci.*, 1985, **155**, 229; (c) J. U. Mack, E. Bertel and F. P. Netzer, *Surf. Sci.*, 1985, **159**, 265; (d) H. Ohtani, R. J. Wilson, S. Chiang and C. M. Mate, *Phys. Rev. Lett.*, 1988, **60**, 2398.
- Review articles: (a) H. Wadepohl, *Angew. Chem.*, 1992, **104**, 253; (b) B. F. G. Johnson, M. Gallup and Y. V. Roberts, *J. Mol. Catal.*, 1994, **86**, 51; (c) H. Wadepohl, *Comments Inorg. Chem.*, 1994, **15**, 369; (d) D. Braga, P. J. Dyson, F. Grepioni and B. F. G. Johnson, *Chem. Rev.*, 1994, **94**, 1585; (e) H. Wadepohl and S. Gebert, *Coord. Chem. Rev.*, 1995, **143**, 535; (f) H. Wadepohl and A. Metz, in *Metal Clusters in Chemistry*, ed. P. Braunstein, L. A. Oro and P. R. Raithby, Wiley-VCH, Weinheim, 1999, vol. 1, ch. 1.15.
- T. Kitamura and T. Joh, *J. Organomet. Chem.*, 1974, **65**, 235.
- H. Wadepohl, S. Gebert, H. Pritzkow, D. Braga and F. Grepioni, *Chem. Eur. J.*, 1998, **4**, 279.
- H. Wadepohl, S. Gebert, R. Merkel and H. Pritzkow, *Chem. Commun.*, 1999, 389.
- H. Wadepohl, S. Gebert, R. Merkel and H. Pritzkow, *Eur. J. Inorg. Chem.*, 2000, 783.
- H. Wadepohl, S. Gebert, H. Pritzkow, D. Osella, C. Nervi and J. Fiedler, *Eur. J. Inorg. Chem.*, 2000, 1833.

- 13 Throughout this paper, the face of the Rh₄ cluster which binds the μ_3 -C₈H₆R₂ ligand will be referred to as the 'basal Rh₃ plane'. The fourth rhodium (and its ligands) is 'apical'.
- 14 G. Deganello, *Transition Metal Complexes of Cyclic Polyolefins*, Academic Press, London, 1979.
- 15 J. C. Green, P. Powell and J. E. van Tillborg, *Organometallics*, 1984, **3**, 211.
- 16 J. Moraczewski and W. E. Geiger, *J. Am. Chem. Soc.*, 1979, **101**, 3007; J. Moraczewski and W. E. Geiger, *J. Am. Chem. Soc.*, 1981, **103**, 4779.
- 17 W. E. Geiger, T. Gennett, M. Grzeszczuk, G. A. Lane, J. Moraczewski, A. Salzer and D. E. Smith, *J. Am. Chem. Soc.*, 1986, **108**, 7454.
- 18 H. Wadepohl, R. Merkel and H. Pritzkow, *Acta Crystallogr., Sect. C*, 1998, **54**, 1095.
- 19 A. K. Smith and P. M. Maitlis, *J. Chem. Soc., Dalton Trans.*, 1976, 1773.
- 20 1,4-(SiMe₃)₂-2,4,6,8-C₈H₈ could also be labelled 1,6-(SiMe₃)₂-1,3,5,7-C₈H₈.
- 21 N. C. Burton, F. G. N. Cloke, S. C. P. Joseph, H. Karamallakis and A. A. Sameh, *J. Organomet. Chem.*, 1993, **462**, 39.
- 22 P. Berno, C. Floriani, A. Chiesi-Villa and C. Rizzoli, *J. Chem. Soc., Dalton Trans.*, 1991, 3085.
- 23 F. G. N. Cloke, J. C. Green, P. B. Hitchcock, S. C. P. Joseph, P. Mountford, N. Kaltsoyannis and A. McCamley, *J. Chem. Soc., Dalton Trans.*, 1994, 2867.
- 24 J. H. Bieri, T. Egolf, W. v. Philipsborn, U. Piantini, R. Prewo, U. Ruppli and A. Salzer, *Organometallics*, 1986, **5**, 2413.
- 25 H. Wadepohl, in *Physical Organometallic Chemistry Vol. 3*, ed. M. Gielen, Wiley & Sons, New York, in print.
- 26 H. Wadepohl, in *The Synergy Between Dynamics and Reactivity at Clusters and Surfaces*, ed. L. J. Farrugia, NATO ASI Series C: Mathematical and Physical Sciences, vol. 465, Kluwer, Dordrecht, 1995, p. 175.
- 27 M. I. Bruce, P. A. Humphrey, B. W. Skelton and A. H. White, *J. Organomet. Chem.*, 1996, **526**, 85.
- 28 K. H. Claus and C. Krüger, *Acta Crystallogr., Sect. C*, 1988, **44**, 1632.
- 29 H. Wadepohl and R. Merkel, unpublished work.
- 30 SHELXS-86, G. M. Sheldrick, *Acta Crystallogr., Sect. A*, 1990, **46**, 467; SHELXL-97, G. M. Sheldrick, Universität Göttingen, Germany, 1997.
- 31 PLATON, A. L. Spek, Utrecht University, Utrecht, The Netherlands, 2001; A. L. Spek, *Acta Crystallogr., Sect. A*, 1990, **46**, C31.
- 32 SCHAKAL-99, E. Keller, Universität Freiburg, Germany, 1999.